

# Kinetics of self-induced aggregation in Brownian particles.

Fabio Cecconi,<sup>1</sup> Giuseppe Gonnella,<sup>2</sup> and Gustavo P. Saracco<sup>3</sup>

<sup>1</sup>*INFN-SMC and Istituto dei Sistemi Complessi ISC-CNR, Via dei Taurini 19, I-00185 Rome Italy.*

<sup>2</sup>*Dipartimento di Fisica, Università di Bari and  
Istituto Nazionale di Fisica Nucleare, Sezione di Bari.  
Via Amendola 173, 70126 Bari Italy.*

<sup>3</sup>*Instituto de Investigaciones Fisicoquímicas Teóricas y Aplicadas (INIFTA).  
UNLP, CONICET. Casilla de Correo 16, Sucursal 4 (1900) La Plata, Argentina.*

We study a model of interacting random walkers that proposes a simple mechanism for the emergence of cooperation in group of individuals. Each individual, represented by a Brownian particle, experiences an interaction produced by the local unbalance in the spatial distribution of the other individuals. This interaction results in a nonlinear velocity driving the particle trajectories in the direction of the nearest more crowded regions; the competition among different aggregating centers generates nontrivial dynamical regimes. Our simulations show that for sufficiently low randomness, the system evolves through a coalescence behavior characterized by clusters of particles growing with a power law in time. In addition, the typical scaling properties of the general theory of stochastic aggregation processes are verified.

PACS numbers: 05., 05.40.-a, 45.70.-n

## I. INTRODUCTION

A process frequently encountered in the study of chemical and physical phenomena is the aggregation of small particles joining each other to form larger spatial structures and clusters. The comprehension of the general properties of aggregation processes constitutes a cross-disciplinary interest for pure and applied research [1, 2, 3, 4, 5, 6] with broad implications to engineering and industrial technology [7].

Aggregation is also a basic process in those biological systems where cooperation activity among individuals usually involves social behaviors. A well known example is *animal grouping* where an ensemble of individuals belonging to the same species live together into organized communities such as insect swarms, mammal herds, fish-schools, and bird flocks [8, 9]. The emergence of cooperation is still one of the most puzzling mechanism occurring in biology, mainly because social and altruistic behaviors are against evolutionary selection which, instead, promotes antagonism and competition. Mathematical population biology [10, 11, 12] and Game Theory [13, 14, 15, 16] have always attempted to reconcile altruism with evolutionary selection trying to establish rigorous and quantitative basis to the emergence of cooperation among individuals. One of the first approaches, known as *kinship theory*, has been elaborated by W.D. Hamilton [17]. It is based on the principle of *kin selection* and allows altruism to arise among siblings provided they share enough common genes. Although the Hamilton's principle strictly works for related individuals, it has been also applied to cases of absence of kin recognition as a rather general explanation for altruism. Alternatively, when genetic arguments cannot be manifestly invoked because cooperation involves unrelated individuals, it is reasonable to resort to minimalist phenomenological models describing the mutual advantage

to form a group or to make coordinated movements [18] in terms of effective “social” interactions. Synchronized and collective behaviors, on the other hand, are the result of “short-” and “long-range” interactions between different units which, in social biological systems, are not very dissimilar to those used in the description of fluids and condensed matter. In this perspective, it is reasonable to hope that some general features of collective behaviors of living organisms can be simulated and classified through the same principles of statistical mechanics successfully applied to understand the structural organization of the matter.

General and simple theoretical descriptions of cooperation in social communities requires two principal ingredients: i) the space of states, where each point represents the status of the individuals and ii) the strategy, that is the rule according to which the individuals (players) decide to change their status in response to partial or complete information about the actions of the other players [16, 19]. The prevalence of cooperation is the outcome of those strategies rewarding altruistic acts and punishing defections. These rules should be given as simple and generic as possible in order to capture the essential and universal aspects of the problem without making the theoretical approach extremely complex or too computationally demanding.

In a previous work [20, 21] we studied a model suggested by Sigmund and Nowak [22] to test the hypothesis of the emergence of cooperation by *indirect reciprocity* among unrelated individuals. In their game theoretical approach, Sigmund and Nowak assumed that cooperation to work in evolved social systems requires the knowledge of “reputation or status” of their members (players). Thus a dynamical coordinate,  $S$ , the *image score*, is assigned to each player signaling his/her reputation or status to the group.  $S$  is updated according to the altruistic or selfish acts made by players in the past and it

is an information accessible to the whole community. At each turn of the game, a randomly selected player with score  $S$  assesses the possibility to provide help only to those opponents with a score greater than  $S$ . The image score, thus, determines the selfish or altruistic strategy. Altruism, despite the cost, is preferable since it increases  $S$  that, conversely, is lowered by a defection. In this scheme, cooperation occurs thanks to the principle “help and you will be helped”.

A simpler version of this problem was recast, in a recent paper [20], in terms of a non-linear Fokker-Planck equation for the population of individuals with a certain image score. The equation had a non-local drift term that characterized the strategy. The peers exert a sort of “pressure” on each other within a finite range of influence in order to uniform their image score to the majority. In this sense, the model produces an aggregation mechanism in the space of scores driven by a population gradient; aggregated states correspond to situations where cooperation is achieved. The model, upon changing the system parameters, exhibited a transition from an aggregation behavior to a uniform state with no prevalence of selected image scoring.

This model, in another context and with proper changes, can also be used to describe pattern formation and chemotaxis phenomena where diffusion competes with a drift induced by chemical or population gradients [23, 24, 25, 26, 27].

In this paper we focus on the dynamics of the aggregation process which was not considered in Ref. [20]. To this aim, we employ a discrete, or individual based, variant of that model, where a set of individuals modify their status according to stochastic differential equations corresponding to a Brownian motion with a drift induced by the spatial distribution of other walkers. This model can also be interpreted as a collection of interacting random walks [28] where the path coalescence depends on the balance between the diffusion and the nonlocal drift. The particle-based modeling permits one to track the state and position of each component of the system. It is appropriate to study the fluctuations in this kind of aggregation dynamics characterized by the formation and merging of growing clusters. We shall see that, differently from previous proposed mechanisms, the coalescence of trajectories does not emerge as a result of direct interactions between particles [29] or via reaction-diffusion mechanism [8], but rather it is the consequence of the drift term sensible to density fluctuations occurring even at distances relatively large. We found that in this model, aggregation and clustering follow the general scaling behavior of stochastic coalescence phenomena [30, 31, 32] with power law for the kinetics of the number and average mass of clusters.

The paper is organized as follows. In sect. II we describe the model and the basic features of its dynamics. Sect. III is devoted to the presentation and discussion of numerical results. Finally, in sect. IV, we draw conclusions.

## II. MODEL OF INTERACTING INDIVIDUALS

The model consists in a system of  $N$  units (individuals) which change their state  $x_i$  according to a sort of majority rule. The variable  $x_i$ , referred to the  $i$ -th member, might indicate the reputation score in indirect cooperation models, the position in a possible chemotaxis description, or some other amplitude characterizing the role of an individual within a population biology framework. Hereafter, without loss of generality, it is convenient to adopt the terminology of spatially distributed systems, thus  $x$  will be a spatial coordinate. The formulation, however, can apply to other and different contexts.

We assume that each individual changes  $x_i$  according to the non-local stochastic equation of motion

$$\dot{x}_i = v(x_i) + \sqrt{2D}\xi_i \quad (1)$$

with the drift  $v$  defined by the formula

$$v(x_i) = \lambda \frac{w_+(x_i, t) - w_-(x_i, t)}{w_+(x_i, t) + w_-(x_i, t)} \quad (2)$$

where  $w_{\pm}$  are given by

$$w_{\pm}(x_i) = \sum_j \Theta[\pm(x_j - x_i)] \exp(-\alpha|x_j - x_i|) \quad (3)$$

The velocity at which an individual “decides” to move to the left or to the right is the result of his perception of the unbalance,  $w_+ - w_-$ , between the populations at his left and right. This perception is simply modeled by the exponential weight with a coefficient  $\alpha = 1/r_0$  that defines the *sensing distance*, *i.e.* the range  $r_0$  within which one individual still perceives the presence and the influence of the other members of the group ( $|x_i - x_j| \leq r_0$ ). This means that, unless  $\alpha = 0$ , only partial information about the population is available to each individual. In this scheme,  $v_i$  is likely to point towards the most populated regions if not too far from the  $i$ -th player; the evolution rule (1,2), therefore, defines an aggregation process where individuals preferably migrate, advected by  $v$ , towards the regions with higher local population.  $\Theta(s)$  is the unitary step function. A random noise  $\xi$  of zero average and correlation

$$\langle \xi_i(t)\xi_j(t') \rangle = \delta_{ij}\delta(t - t')$$

incorporates some degree of uncertainty or randomness in the dynamics of the system, introducing the possibility for the individuals to change even randomly their state. In a possible chemotaxis framework [23], the system (1,2) represents the motion of biological organisms that, while performing a random walk with diffusion coefficient  $D$ , secrete pheromones whose concentration turns to be proportional to the number of individuals at a given place. Then, the organisms following the concentration gradient feel an attraction towards the nearest most crowded zones [33]. The parameter  $\lambda$  sets the range of the velocity excursion; the normalization factor  $w_+(x_i) + w_-(x_i)$

in Eq. (2) makes the velocity bounded within  $[-\lambda, \lambda]$  implying that individuals have a limited response velocity as it happens in realistic cases. This maximal speed is reached when  $w_+(x_i) = 0$  or  $w_-(x_i) = 0$ , *i.e.* when the whole population lies completely on the right/left with respect to  $x_i$ . The  $i$ -th individual, then, will move ballistically with the absolute maximal velocity  $|v_i| = \lambda$  to join the other  $N - 1$  members independently of  $N$ . Thus the drift  $v(x_i)$  is a nonextensive parameter defining the model. Equation (1) can be cast in a dimensionless form with the proper rescaling of time  $t \rightarrow t/(\alpha\lambda)$  and space  $x \rightarrow x/\alpha$ , where only one independent parameter survives. In the natural units ( $\alpha = \lambda = 1$ ), the variance of the noise is renormalized to  $D \rightarrow \alpha D/\lambda$  [20]. Hereafter therefore we work with the values  $\alpha = \lambda = 1$ .

In our study, we consider the effects of varying both the randomness and the density of individuals in order to see how they affects the kinetics of aggregation. For low noise levels ( $D < D_c$ ) the system has a strong propensity to aggregation and almost independently of the initial conditions the particles form clusters that collapse each other to generate new larger clusters. Figure 1 provides some instances of the basic phenomenology of the system dynamics, for  $D = 0$ ,  $D = 0.1$ ,  $D = 0.5$  and  $D = 1$ .

In small systems, the process continues until only one cluster survives with a well defined size and particle distribution [20]. However, in larger systems  $N \rightarrow \infty$  with random initial configuration, this final state is practically inaccessible to simulations because the transient regimes become extremely long. In this case the aggregation kinetics is the dominating and relevant feature of the system behavior.

For  $D > D_c$ , the dynamics of the system loses its tendency to cluster and particles basically perform a standard random walk inside the one-dimensional box containing them. This kind of non-equilibrium transition is clearly illustrated by figure 2 where we plot the evolution of the number of clusters  $N_c$  that are present in the system. We define a cluster as a set of particles with mutual distances  $|x_i - x_j|$  below a given cutoff  $\varepsilon$  that we shall call resolution. We see that for noise below  $D_c = 1$ ,  $N_c$  fluctuates but exhibits a decreasing trend in time, signaling that clusters coalesce with each other so their average number decreases.

If  $D > D_c$ , after a small transient, the number of cluster fluctuates around a stationary value. A similar behavior is observed in *spreading* experiments where the system evolves from a set of spatially localized initial conditions. This kind of numerical simulations requires no boundary conditions to let the system free to occupy a broader and broader portion of the x-axis. The time evolution of the variance of the system with respect to its center of mass

$$R(t) = \frac{1}{N^2} \sum_{i,j>i} \langle [x_i(t) - x_j(t)]^2 \rangle \quad (4)$$

is shown in Fig. 3 for different values of  $D$  and averaged over independent runs. Upon rising  $D$  from zero,  $R(t)$  displays a crossover from a regime in which it decreases

with time or remains bounded to a regime where spreading occurs as  $R(t)$  grows with time from the initial value  $R(0) = \sigma_0^2$ . This basically confirms the scenario already described for the number of clusters: when the dynamics is dominated by noise effects, the clusters become unstable and evaporate.

The picture emerging from the simulations on the existence of the bifurcation point  $D_c = 1$  is affected by finite size effects allowing only an approximate identification of  $D_c$ . However, the presence of a transition at the exact value  $D_c = 1$  can be supported by the following analysis [20]. It is convenient to consider the Fokker-Planck (FP) equation associated to the Langevin equation (1) and observe that the latter can be derived formally from a local potential  $U(x_i) = -\ln\{\phi(x_i)\}$ ,

$$\dot{x}_i = -\frac{\partial U(x_i)}{\partial x_i} + \sqrt{2D}\xi_i = \frac{1}{\phi(x_i)} \frac{\partial \phi(x_i)}{\partial x_i} + \sqrt{2D}\xi_i \quad (5)$$

where

$$\phi(x_i) = \sum_{j \neq i} \exp(-|x_j - x_i|)$$

and  $D$  indicates the renormalized noise variance. In limit of large number of particles and in the mean-field like approach, the sum over  $j$  can be replaced by an integral involving the single particle density  $\rho(x, t)$ ,

$$\phi(x, t) = \int dy \rho(y, t) e^{-|y-x|}. \quad (6)$$

This formula clarifies that the dynamics of each walker can be regarded as it occurs in a time dependent mean potential generated by the local environment produced by the position of the other walkers. The integral equation (6) can be transformed into a differential equation for  $\phi$  by a double differentiation of both members

$$\partial_x^2 \phi(x, t) - \phi(x, t) = -2\rho(x, t). \quad (7)$$

The FP equation governing the evolution of the density of particles obeying Eq. (5) is

$$\partial_t \rho = -\partial_x(\rho/\phi \partial_x \phi) + D \partial_x^2 \rho. \quad (8)$$

It admits a stationary implicit solution  $\rho_s(x) = C[\phi_s(x)]^{1/D}$  with  $C$  a positive integration constant determined by the normalization of  $\rho$ . The solution has to be made explicit through the substitution  $\rho_s(x)$  into Eq. (7),

$$\phi_s'' - \phi_s = -2C\phi_s^{1/D}$$

that integrated after a multiplication for  $\phi_s'$  of both members yields

$$\frac{1}{2}\phi_s'^2 - \frac{1}{2}\phi_s^2 + \frac{2DC}{1+D}\phi_s^{1+1/D} = E, \quad (9)$$

with  $E$  being another integration constant. The normalizability of  $\rho_s(x)$  and, as a consequence, of  $\phi_s(x)$  for infinite systems requires that  $\phi$  vanishes enough faster when

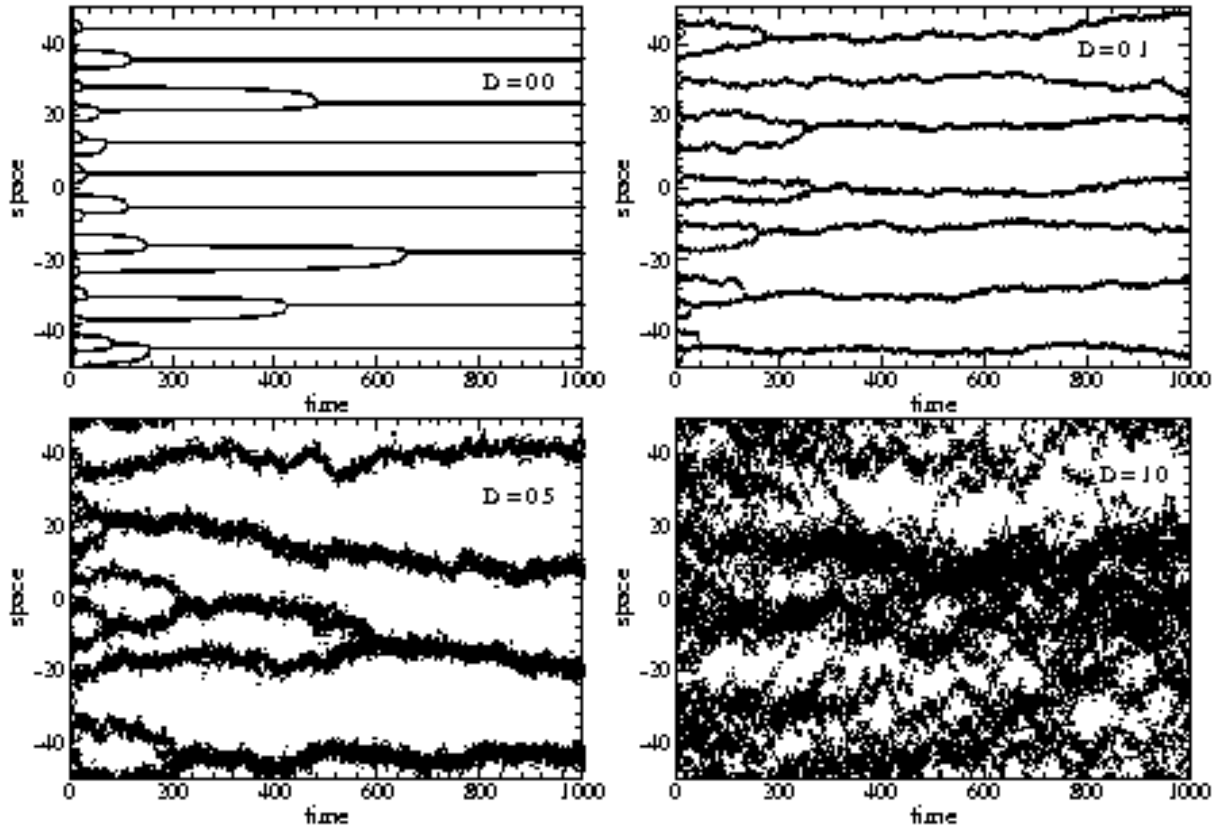


FIG. 1: Trajectories of  $N = 100$  particles obtained by numerical integration of Eq. (1) with time-step  $h = 0.01$ , starting from uniformly distributed initial conditions in a range  $L = [-50, 50]$ . The four panels, referring to parameters  $\alpha = 1$ ,  $\lambda = 1$  and noise  $D = 0$ ,  $D = 0.1$ ,  $D = 0.5$  and  $D = 1$ , show the influence of the randomness on the system phenomenology. True path coalescence is observed only for  $D < 1$ .

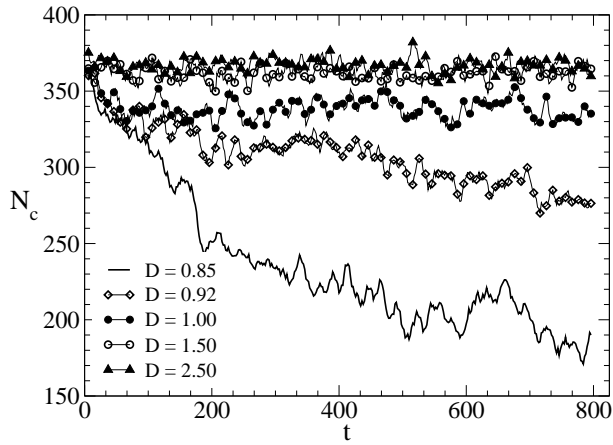


FIG. 2: Evolutions of the number of clusters formed in a system with density  $\rho = 10$  and different variance  $D$  of the noise, indicated in the inset. The threshold  $D_c = 1$  separates aggregation from uniform distribution of particles.

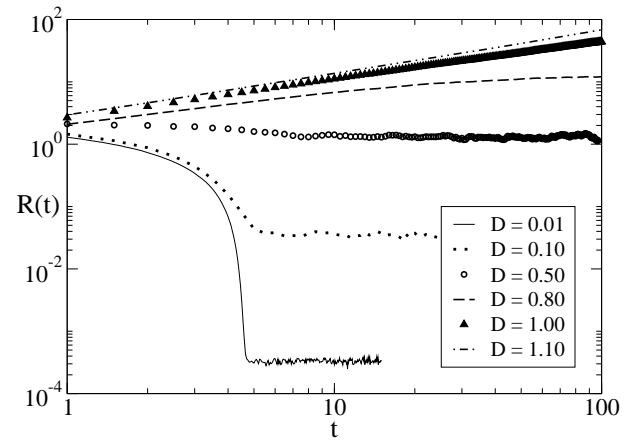


FIG. 3: Log-log plot of the system variance  $R$  versus time in spreading experiments with  $N = 500$  particles at different noise level showing the crossover from localized to delocalized evolutions. Each curve is the result of the average over 200 independent runs.

$x \rightarrow \pm\infty$  implying that  $E = 0$ . Equation (9), provided that  $x$  is interpreted as a time coordinate, corresponds to

the motion of a particle with unitary mass in a potential

$$V_p(\phi_s) = -\frac{1}{2}\phi_s^2 + \frac{2DC}{1+D}\phi_s^{1+1/D}.$$

The properties of  $V_p$  explain the presence or absence of coalescence. Indeed, when  $D > 1$  the motion along the orbit  $E = 0$  reduces to the fixed point  $\phi_s(x) = 0$  [ $\rho_s(x) = 0$ ], while nonzero and localized solutions  $\phi_s(x)$  can be found only for  $D < 1$ . This indicates the presence of a change in the system behaviour occurring when  $D$  goes through the critical point  $D_c = 1$ .

A linear stability analysis over the nonlinear FP equation leads to the same conclusion. Let  $\delta\rho(x, t) = \exp(ikx - \mu t)$  a spatially modulated perturbation of vector  $k$  over a uniform density background. A substitution into the integral (6) gives  $\phi(x, t) = \exp(ikx)/(1 + k^2)$  that, in turn, plugged in the FP equation determines the simple condition  $\mu = k^2(D - 1)$ . Then the perturbation  $\delta\rho$  is exponentially reabsorbed in time for  $D > 1$  so that the uniform state is stable, whereas for  $D < 1$  the perturbation is unstable signaling drastic changes in the system evolution.

In the following we shall focus on the characterization of the aggregation dynamics for  $D < D_c$  by monitoring and quantifying the properties of the clustering kinetics resulting from path coalescence.

### III. AGGREGATION DYNAMICS

We study the dynamics of the system via simulations of Eqs. (1) and (2) numerically integrated through standard second order Runge Kutta algorithm for stochastic equations [34]. All of our simulations, unless differently indicated, started from disordered uniform configurations with particles contained in a one-dimensional box of a fixed size  $L$ . We used a time step  $h = 0.01$ , which is a fair compromise between statistical accuracy of the algorithm and the length of simulations. In the range of explored parameters we verified that a refinement of the time step does not affect the results. During the runs, when a particle close to the boundaries escapes the box, it is reinjected on the other side. Such reinjection events are rare because, in the noise range we worked, the drift term (2) is dominant and the particles close to the boundaries move preferentially towards the bulk of the systems; thus border effects are really irrelevant. However, to check that the results are not affected by the re-injection through the boundaries, we repeated some of the simulations with fully periodic boundary conditions (*i.e.*, considering system on a ring of length  $L$ ). The different implementation of the boundary conditions did not alter the results. In the periodic boundary conditions the left and right position with respect to an individual located at  $x_i$  is specified by considering that each individual divides the ring in two halves of length  $L/2$  each, accordingly, all individuals laying on the left or on the right of  $x_i$  can be identified without ambiguity.

In this section, we analyze and characterize the aggregation kinetics observed in the system simulations at low noise regimes, where the dynamics is dominated by the drift term. As shown in Fig. 1, aggregation starts by forming small clusters which, in turn, collide and merge to generate larger and larger structures. The larger clusters exhibits low coalescence rates and acts as coagulation centers by absorbing single particles or smaller clusters.

A first quantitative attempt to describe the aggregation kinetics can be made by the following argument that considers the very ideal case of only two clusters, approximated as flat particle distributions in the intervals  $[X_i - \delta/2, X_i + \delta/2]$  around their centers of mass  $X_i$  ( $i = 1, 2$ ). By assuming that they attract each other without changing too much of their structure, the average distance between the centers of mass  $\Delta = X_2 - X_1$  contracts in time according to the equation (see the Appendix A):

$$\dot{\Delta} = -\frac{2}{1 + b \exp(\Delta)} \quad (10)$$

where  $b$  is a parameter depending on the cluster geometry, in the specific case  $b = 2/\{1 + \exp(\delta/2)\}$ ;  $b$  can also be interpreted as a tunable parameter of a fitting procedure. In this ideal situation, the mean spreading, Eq. (4), verifies the relation  $R(t) = \Delta^2(t)/4$ . In Fig. 4, we plot the theoretical spreading  $R(t)$  obtained by the integration of Eq. (10) along with the corresponding result extracted from simulations on a system with density  $\rho = 10$ ,  $N = 100$  particles and starting from random configurations. We observe the formation of few clusters that relatively soon coalesce,  $\Delta \sim 0$ , with a behavior quite in agreement with that suggested by Eq. (10).

However, simulations performed on larger systems to improve the clustering statistics revealed a rate of aggregation different from that expected from Eq. (10) that basically applies only to binary collisions. We, therefore, investigated systematically the aggregation process through a set of simulations on a system involving  $N = 10^4$  particles, where we monitored the time evolution of the standard indicators used to quantify the degree of clustering in aggregating systems [35, 36]. Such indicators display a trivial behavior when the noise level is  $D > D_c$ , as expected because uniform particle distributions there occur.

We measured the number of clusters  $N_c(t)$ , their average mass  $M_c(t)$ , and the distribution  $P_t(m)$  representing the number of clusters with size  $m$  at time  $t$ . We also considered the average distance  $\Delta(t)$  between neighbor clusters which provides information about the spatial compactness of the system. Such quantities were averaged over a set of independent runs starting from random particle distributions with a given density.

In all the cases considered we observed (see Fig. 5) the algebraic decay of the cluster number  $N_c$  according to

$$N_c(t) \sim t^{-z}. \quad (11)$$

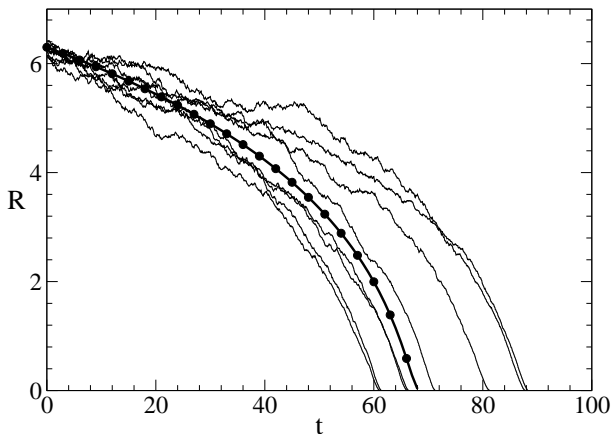


FIG. 4: Time behavior of  $R(t)$  [Eq. 4] for a system with  $N = 100$  particles, uniformly distributed with density  $\rho = 10$  and  $D = 0.01$ . The pointed line indicates the corresponding quantity obtained by the numerical solution of the differential Eq. (10).

Each cluster has a characteristic size and a typical distribution of particles that depend on the noise and the other parameters in agreement with the analytical result for the stationary single cluster distribution derived in Ref. [20]. This suggests that, when sufficiently isolated, a cluster persists over a longer period in a sort of quasi-equilibrium state.

The results from Fig. 5, referring to systems with different densities  $\rho$  but same noise  $D = 0.05$ , suggest an exponent  $z$  close to 0.2, independent of  $\rho$  within statistical errors. We also observed systematically that, at each time  $t$ , the larger the density the lower the number of clusters. This means that systems with higher densities generate a smaller number of clusters that, due to the conservation of the number of particles, must contain a larger number of particles already in the first stages of their formation. The density therefore sensibly affects only the initial rate of cluster formation, that is, at higher densities clusters form faster. Later on, different densities reflect only in different prefactors of the power law (11). This also implies that, when working at too high densities, cluster statistics becomes worse and the power-law equation (11) cannot be clearly detected.

A straightforward consequence of the conservation of the particle number and of the decay (11) is that the average cluster mass  $M_c$  grows with the inverse power law  $M_c \sim t^z$ , as verified in our simulations (not shown for the sake of space). In figure 6, we plot the average distance between nearest neighbor clusters  $\Delta$  directly extracted from the runs. Obviously, this quantity also exhibits the scaling

$$\Delta(t) \sim t^z \quad (12)$$

with the same exponent  $z$  of the mean cluster mass. The presence of such a power law seems to indicate that as the process keeps going on and a reasonable number of larger

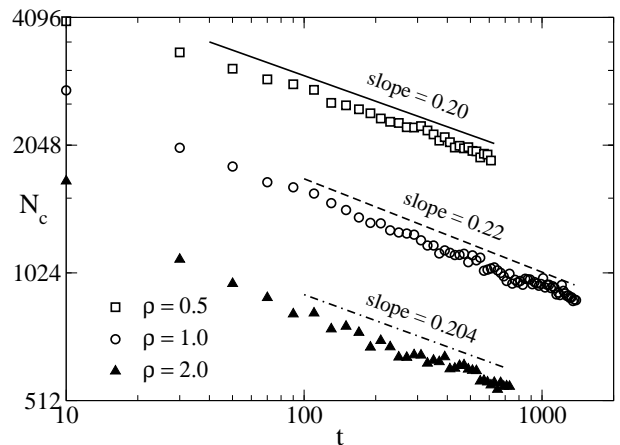


FIG. 5: Power law decay in time of the average number clusters  $N_c$ . Data refer to noise  $D = 0.05$  and to the three densities indicated in the inset. Lines indicate the best fit to data whose slopes are the exponent  $z$ . The resolution is  $\varepsilon = 0.1$  in all cases.

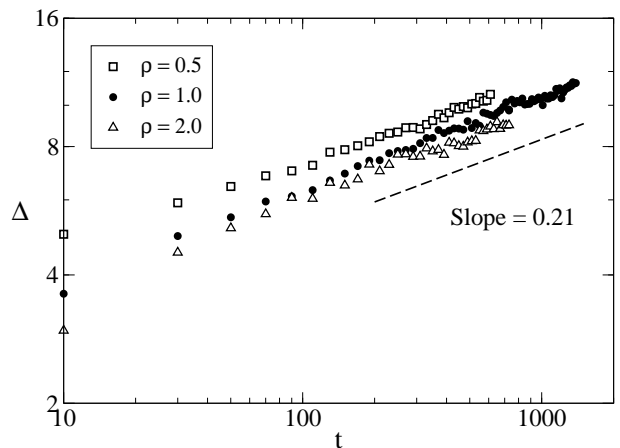


FIG. 6: Time-behavior of the average distance between clusters for different particle density, for a system with noise  $D = 0.05$ . The resolution is  $\varepsilon = 0.1$  in all cases, however, the same data processed with resolution  $\varepsilon = 0.5$  gave the same exponent within statistical errors.

clusters is formed, further aggregation is suppressed and cluster growth becomes very slow. We also checked the dependence of  $z$  on the noise strength  $D$ . Fluctuations induced by the high noise, indeed, produce fragmentation or evaporation of particles from already formed clusters, making the influence of  $D$  on  $z$  more relevant than that of  $\rho$ . Figure 7 reports data on the variation of the slope [Eq. (12)] at different  $D$  and indicates that, although the power law behavior remains robust with respect to  $D$ , until  $D < D_c$ , the  $z$  exponent lowers as  $D$  approaches from below the critical value  $D_c$ . Therefore, in the region of parameter we explored, the simulation results indicate that the value of the exponent  $z$  weakly depends on the density but it is quite sensitive to the noise level  $D$ .

To investigate in more details the aggregation process

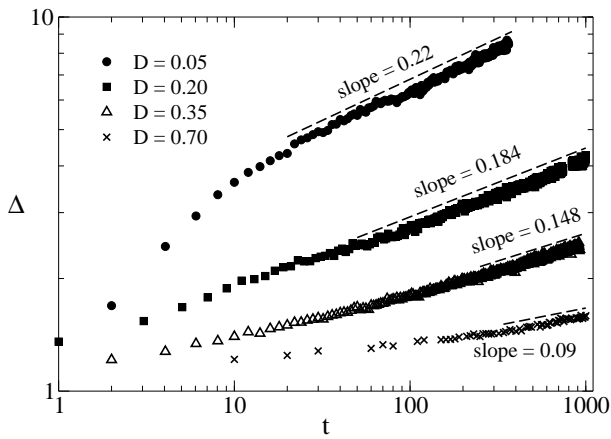


FIG. 7: Power-law behavior with time of the average cluster distance for a system with  $N = 10^4$  particles and different noise levels  $D$  at the same density  $\rho = 1.0$  and resolution  $\varepsilon = 0.1$ .

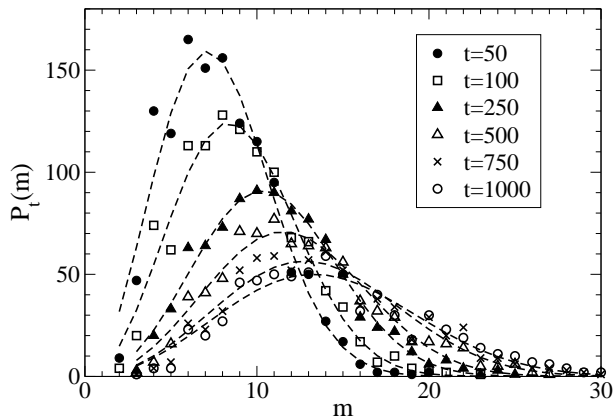


FIG. 8: Time-dependent histograms of the cluster masses collected from simulations of a system of  $N = 10^4$  particles, density  $\rho = 1.0$ , and  $D = 0.05$ . Lines are guides for the eye.

we collected the histograms of the cluster masses at different times during the runs. The evolution of mass distribution is shown in figure 8 at density  $\rho = 1$  and  $D = 0.05$ . The shape of the distribution, at earlier times, rises sharply at small values of  $m$ , from zero to a maximum and then decays mildly to zero at larger masses. The distribution are skewed and peaked around the average and their tails are not very extended. As time goes on, the average increases and the distributions become broader with tails that spread over larger interval of masses  $m$ , indicating a clustering activity that involves polydispersity in cluster size. Basic theories for aggregation phenomena [37] suggest the scaling symmetry

$$P_t(m) \sim M_c^\theta f(m/M_c) \quad (13)$$

for cluster mass distributions for processes occurring with an asymptotically well-defined average size  $M_c$  for the aggregates. The constraint of the total mass (number of

particle) conservation,

$$N = \sum_m m P_t(m),$$

sets the scaling exponent to the value  $\theta = -2$  [31, 32, 38]. The rescaling of distributions in Fig. 8, according to Eq. (13), yields the data collapse shown Fig. 9 in linear (top) and linear-log (bottom) plots.

The collapse is rather satisfactory both for the bulk and tails of the distributions and fully consistent with the power-law behavior of  $N_c(t)$ . In fact, as an immediate consequence of the scaling form (13), it is straightforward to verify that, in the continuum limit and with the change of variable  $m \rightarrow m/M_c$ , we obtain

$$N_c(t) = \sum_m P_t(m) \sim M_c(t)^{-1},$$

*i.e.*, the number of clusters is proportional to the inverse of their average mass  $M_c$ . This analysis shows that our model, although not directly related to general stochastic aggregation processes [40], follows their typical scaling behavior.

#### IV. CONCLUSIONS

In this paper we considered a one-dimensional model that promotes aggregation of particles for a certain range of the parameters. The model, related to a certain class of problems concerning the onset of social behavior among individuals, is defined by a first order stochastic differential equation. More specifically, each Brownian particle, representing a living organism, undergoes a drift velocity depending nonlocally on the other particle positions. This drift is the response to the population unbalance perceived by a single individual between left and right. Local fluctuations occurring in the population density determine a displacement towards the regions with the highest crowding. However, a limited sensing range of the individuals, mimicked in the model by an exponential weight in the distance, prevents them from reacting to fluctuation events occurring too far. The competition between far large and near, but small, aggregating centers makes the system dynamics nontrivial. Below a certain randomness threshold  $D_c = 1$ , aggregation of particles in clusters of increasing size is observed, but at higher noise the organisms disperse via almost independent random walks suppressing social behavior.

The aggregation process has been investigated through a set of simulations where we monitored the time behavior of the standard indicators used to quantify the degree of clustering in aggregating systems [35, 36]. Such indicators of course display a trivial behavior when the noise exceeds the threshold  $D_c$  because uniform particle distributions occur. On the contrary they exhibit a power-law behavior at low noise regimes showing that this model obeys the typical scaling behavior of stochastic aggregation processes. However the relevant role of

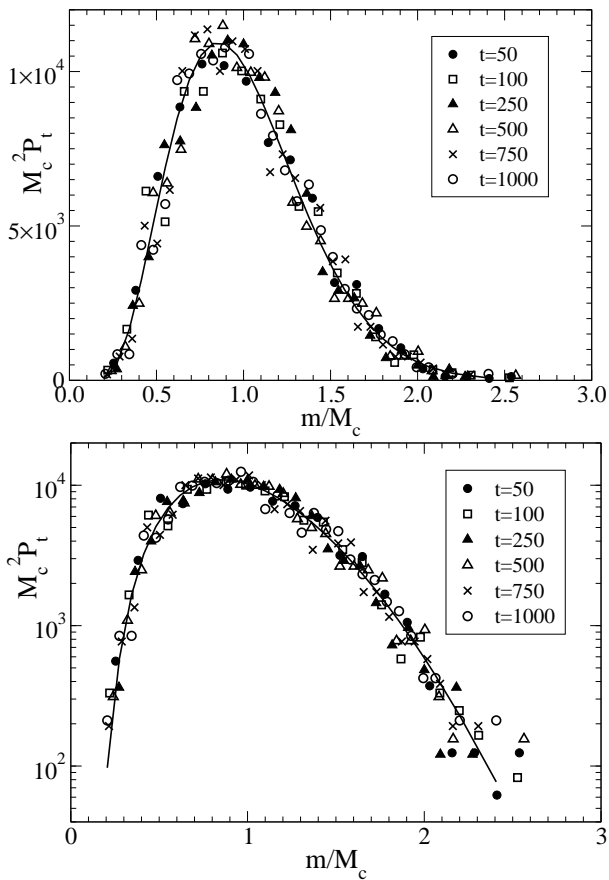


FIG. 9: Data collapse of the time dependent distributions shown in Fig. 8 obtained through the rescaling suggested by Eq. 13: linear-linear (top) and linear-log (bottom) plots. The solid line represents the fitting curve  $f(x) = a_0 x^{-2} \exp\{a_1/x - a_2 x^2\}$ .

the spatial fluctuations, as already noted for other processes Ref. [39], does not allow one to explain the exponents through the mean field theory defined by the Smoluchowsky equation for coagulation [40].

### Acknowledgments

G.G. acknowledges the support by MIUR (PRIN 2004). G.P.S. acknowledges the support of CONICET. We are indebted to Amos Maritan, Matteo Marsili, Massimo Cencini and Paolo da Pelo for useful discussions and suggestions.

### APPENDIX: A

In this appendix we show how to derive the evolution equation (10) for the centers of mass  $X_1$  and  $X_2$  of two

aggregates, each containing half of the particles  $N/2$ . We assume that this situation roughly corresponds to a particle distribution with density

$$\rho(y, t) = \rho_0 \{ \Theta[\delta^2/4 - (y - X_1)^2] + \Theta[\delta^2/4 - (y - X_2)^2] \}$$

where  $\rho_0 = N/(2\delta)$ ,  $\Theta(u)$  indicates the unitary step function and  $\delta$  represents the spatial extension of the two aggregates. Furthermore, we suppose that the intra-cluster dynamics is basically frozen. Therefore, each cluster travels as a rigid body maintaining its shape basically unchanged, so that the relevant time dependence lies only in their center mass positions  $X_1(t)$  and  $X_2(t)$ . This density produces a drift velocity that can be derived from the integral (6)

$$\phi(X_1) = \int_{X_1 - \delta/2}^{X_1 + \delta/2} dy e^{-(y - X_1)} + \int_{X_2 - \delta/2}^{X_2 + \delta/2} dy e^{-(y - X_1)},$$

then

$$\phi(X_1) = 2(1 - e^{-\delta/2}) + 2 \sinh(\delta/2) e^{X_1 - X_2}.$$

According to Eq. (5), the velocity of cluster 1 reads

$$V_1 = \frac{\phi'(X_1)}{\phi(X_1)} = \frac{\sinh(\delta/2) e^{X_1 - X_2}}{(1 - e^{-\delta/2}) + \sinh(\delta/2) e^{X_1 - X_2}},$$

that, after some algebraic manipulations simplifies to

$$V_1 = \frac{1}{1 + b e^{X_2 - X_1}} \quad (\text{A.1})$$

with  $b = [1 - \exp(\delta/2)] / \sinh(\delta/2) = 2/[1 + \exp(\delta/2)]$ . The velocity of the second cluster, due to the symmetry of the problem, has to be  $V_2 = -V_1$ , so that the relative velocity of the two rigid clusters is  $-2V_1$ , that is Eq. (10) providing that  $\Delta = X_2 - X_1$ . More generally, we can observe that for two very localized aggregates of sizes  $\delta_1$  and  $\delta_2$  with local density  $\rho_1$  and  $\rho_2$ , respectively, the integrals contributing to  $\phi$  can be roughly approximated to  $\rho\delta$ , the cluster relative velocity is thus estimated as

$$V_r = 2 \frac{\rho_2 \delta_2 e^{-\Delta}}{\rho_1 \delta_1 + \rho_2 \delta_2 e^{-\Delta}} = \frac{2}{1 + b e^{\Delta}}.$$

The parameter  $b = \rho_1 \delta_1 / (\rho_2 \delta_2)$  thus represents a measure of the relative weights of the two clusters.



- 
- [1] H.R. Pruppacher and J.D. Klett, *Microphysics of Clouds and Precipitation* (Kluwer Academic: Dordrecht, The Netherlands, 2003).
- [2] P.J. Flory, *Principles of Polymer Chemistry*. (Cornell University Press, London, 1953).
- [3] H.M. Jaeger and S.R. Nagel, *Rev. Mod. Phys.* **68**, 1259 (1996).
- [4] M. Wilkinson and B. Mehlig, *Phys. Rev. E* **68**, 040101R (2003).
- [5] J. Bec, A. Celani, M. Cencini and S. Musacchio, *Phys. Fluids* **17**, 073301 (2005).
- [6] P. Peebles, *The large scale structure of the universe*, (Princeton University Press, Princeton, NJ 1980).
- [7] M. Elimelech, X. Jia, J. Gregory and R. Williams, *Particle Deposition and Aggregation: Measurement, Modelling and Simulation* (Butterworth-Heinemann, Washington DC, 1998).
- [8] A. Okubo and S.A. Levin, *Diffusion and Ecological Problems: Modern Perspectives*. (Springer, New York, 2001).
- [9] G. Flierl, D. Grunbaum, S. Levin, and D. Olson, *J. Theor. Biol.* **196**, 397 (1999).
- [10] S.A. Levin, B. Grenfell, A. Hastings, and A.S. Perelson, *Science* **275**, 334 (1997).
- [11] M.A. Nowak, S. Bonhoeffer, and R.M. May *Proc. Natl. Acad. Sci. USA*, **91**, 4877 (1994); *ibid.* *Nature (London)* **379**, 126 (1996).
- [12] M.W. Hirsch, *Nonlinearity* **1**, 51 (1988).
- [13] R. Axelrod and W.D. Hamilton, *Science* **211**, 1390 (1981).
- [14] M. Mesterton-Gibbons and L.A. Dugatkin, *Quarterly Rev. Biol.*, **67** 267 (1992).
- [15] M. Nakamura, H. Matsuda, and Y. Iwasa, *J. Theor. Biol.* **184** 65 (1997).
- [16] J.M. Smith *Evolution and the Theory of Games*, (Cambridge University Press, Cambridge 1982).
- [17] W.D. Hamilton, *J. Theor. Biol.* **7**, 1 (1964); **7**, 17 (1964).
- [18] T. Vicsek, A. Czirók, E. Ben-Jacob, I. Cohen and O. Shochet, *Phys. Rev. Lett.* **75**, 1226 (1995); G. Gegrégoire, H. Chaté, and Y. Tu, *Physica D* **181**, 157 (2003).
- [19] A. Lotem, M.A. Fishman, and L. Stone, *Nature (London)* **400**, 226 (1999).
- [20] F. Cecconi, M. Marsili, J.R. Banavar, and A. Maritan, *Phys. Rev. Lett.* **89**, 088102 (2002).
- [21] F. Cecconi, J.R. Banavar and A. Maritan *Phys. Rev. E* **62**, R5879 (2000).
- [22] M.A. Nowak and K. Sigmund, *Nature (London)* **393**, 573 (1988).
- [23] J.D. Murray, *Mathematical Biology*, (Springer-Verlag, Berlin 1993).
- [24] M.R. D'Orsogna, M.A. Suchard, and T. Chou, *Phys. Rev. E* **68**, 021925 (2003).
- [25] E. Hernandez-Garcia and C. Lopez *Phys. Rev. E*, **70** 016216, (2004); C. Lopez, E. Hernandez-Garcia, *Physica D* **199**, 223 (2004).
- [26] W. Falk, R.H. Goodwin Jr., and E.J. Leonard *Immunol. Methods* **33**, 239 (1980).
- [27] H.C. Berg and D.A. Brown, *Nature (London)* **239**, 500 (1972).
- [28] J.A. Byers, *Ecology* **82**, 1680 (2001).
- [29] P.H. Chavanis and C. Sire, *Phys. Rev. E* **70**, 026115 (2004); C. Sire and P.H. Chavanis, *Phys. Rev. E* **69** 066109 (2004).
- [30] T. Vicsek and F. Family, *Phys. Rev. Lett.* **52**, 1669 (1984).
- [31] F. Leyvraz, *Phys. Rev. A* **29**, 854 (1984).
- [32] K. Kang and S. Redner, P. Meakin and F. Leyvraz, *Phys. Rev. A* **33**, 1171 (1986).
- [33] E. Keller and A. Segel, *J. Theor. Biol.* **26**, 399 (1970).
- [34] R. Honeycutt, *Phys. Rev. A* **45**, 600 (1992).
- [35] A. Puglisi, F. Cecconi and A. Vulpiani *J. Phys.: Condens. Matter* **17**, S2715 (2005).
- [36] S. Torquato, *Random Heterogeneous Materials: Microstructure and Macroscopic Properties*, (Springer-Verlag, New York, 2002).
- [37] See, e.g., M.H. Ernst, in *Fundamental Problems in Statistical Physics VI*, edited by E.G.D. Cohen (Elsevier, New York, 1985).
- [38] P.G.J. van Dongen and M.H. Ernst, *Phys. Rev. Lett.* **54**, 1396 (1985).
- [39] S.M. Dammer and D.E. Wolf, *Phys. Rev. Lett.* **93**, 150602 (2004).
- [40] M. von Smoluchowski, *Phys. Z.* **17**, 593 (1916).